



A dynamic signal coordination control method for urban arterial roads and its application *

Guo-jiang SHEN^{†1}, Yong-yao YANG²

⁽¹⁾College of Computer Science and Technology, Zhejiang University of Technology, Hangzhou 310014, China)

⁽²⁾Zhejiang Zheda Supcon Information Technique Co., Ltd., Hangzhou 310053, China)

[†]E-mail: gjshen1975@zjut.edu.cn

Received July 19, 2015; Revision accepted Apr. 18, 2016; Crosschecked Aug. 9, 2016

Abstract: We propose a novel dynamic traffic signal coordination method that takes account of the special traffic flow characteristics of urban arterial roads. The core of this method includes a control area division module and a signal coordination control module. Firstly, we analyze and model the influences of segment distance, traffic flow density, and signal cycle time on the correlation degree between two neighboring intersections. Then, we propose a fuzzy computing method to estimate the correlation degree based on a hierarchical structure and a method to divide the control area of urban arterial roads into subareas based on correlation degrees. Subarea coordination control arithmetic is used to calculate the public cycle time of the control subarea, up-run offset and down-run offset of the section, and the split of each intersection. An application of the method in Shaoxing City, Zhejiang Province, China shows that the method can reduce the average travel time and the average stop rate effectively.

Key words: Urban arterial, Control subarea, Coordination control, Correlation degree, Fuzzy logic, Intelligent transportation
<http://dx.doi.org/10.1631/FITEE.1500227>

CLC number: TP273; U491

1 Introduction

As the number of vehicles grows continuously and the need for mobility increases rapidly, traffic congestion and vehicle exhaust pollution are becoming increasingly severe in most cities. As the main transportation roads inside a city, urban arterial roads bear the main traffic load. By coordinating all the traffic signal controllers on an arterial route, traffic signals can be controlled effectively to increase the road's traffic service level, and reduce the average vehicle delay and stop rate. Thus, a carefully designed coordination control system for urban arterial roads

would be of great significance to improve the traffic conditions of the entire city.

As a special case of the road network coordination control paradigm, research on urban arterial coordination control systems and techniques has attracted great interest recently, and many research results have found successful applications. Lee and Lee-Kwang (1999) presented a fuzzy controller for a set of intersections with dynamic traffic patterns, and reported satisfactory performance. Pillai *et al.* (1998) developed a restricted branch-and-bound approach for generating the maximum bandwidth signal timing plans. By extending the MAXBAND program, Gartner and Stamatiadis (2004) obtained an enhanced multi-bandwidth traffic signal setting optimization program. Kong *et al.* (2011) proposed an intelligent coordination control system for urban arterial traffic to achieve two-directional green wave passage with fast speed, leading to highly efficient use of the green signal time. Shen and Kong (2009) presented a traffic coordination control system for a road network,

* Project supported by the National Natural Science Foundation of China (No. 61174174), the Science and Technique Program of Zhejiang Province, China (No. 2015C31059), and the Science and Technique Program of Zhejiang Provincial Department of Transportation, China (No. 2014T08)

ORCID: Guo-jiang SHEN, <http://orcid.org/0000-0003-1064-1250>

© Zhejiang University and Springer-Verlag Berlin Heidelberg 2016

which realized vehicle coordination control and bus prioritization simultaneously. Many new methods for optimizing the signal timing controls of urban traffic networks have been presented, and some have been applied effectively (Lertworawanich *et al.*, 2011; Kong *et al.*, 2013; Kumar *et al.*, 2014; Tettamanti *et al.*, 2014; Febbraro *et al.*, 2015; Wu *et al.*, 2015).

In most cities in China, congenital deficiencies in city planning coupled with an irrational urban layout have often led to an imbalance of traffic flow distribution. Moreover, traffic flow efficiency is much reduced because of multiple intersections between arterial roads and secondary roads or minor branches. Signal coordination control may be one method for effectively solving this problem. However, a conventional coordination control scheme, in which the whole arterial route is treated as a single coordination system, might not necessarily improve traffic flow efficiency, because a coordination control scheme generally requires a single common signal cycle time among all intersections in the coordinated system.

We propose a new dynamic signal coordination control method for urban arterial roads. The control area of the entire arterial road is divided into a number of control subareas according to the correlation degree among adjacent intersections, and then the signal coordinated control is applied to each subarea as a unit. All intersections in each control subarea share the same signal cycle time.

2 Overall coordination framework

A typical urban arterial route consisting of N sequential intersections is shown in Fig. 1. The south–north road is the arterial route and the east–west roads are the secondary roads or branches. The traffic volume is generally much larger on the arterial route. The southbound direction on the arterial road is defined as the up-run direction and the

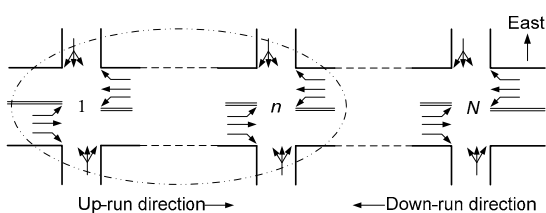


Fig. 1 Sketch of an urban arterial road

northbound direction as the down-run direction. Intersections 1 to n circled by the dotted-line ellipse constitute a control subarea. The goal of coordination control is to ensure a smooth traffic flow in the control subarea, so that most vehicles in the east–west direction can pass through all intersections of the control subarea without stopping, and the green wave bandwidth remains a relatively large value.

The entire system framework includes a control subarea division module and a coordination control module (Fig. 2). The control subarea division module has two functions: calculating the correlation degree between two adjacent intersections, and allocating all intersections of the arterial road to different control subareas according to the calculated correlation degrees. If there is only one intersection in a resulting subarea, the subarea control is reduced to an adaptive control for an isolated intersection (Shen and Sun, 2002). Otherwise, the signals of all the intersections in a control subarea should be manipulated by the dynamic coordination control technique we proposed.

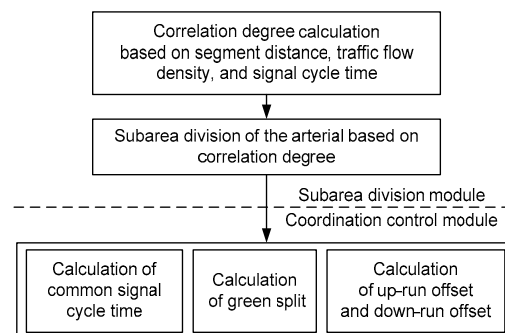


Fig. 2 Framework for the coordination control method

3 Division of control areas

The correlation degree between two adjacent intersections is calculated based on the relevant road section and traffic information, and then the arterial road is divided into a number of control subareas according to the correlation degree. Since the global traffic information of the entire arterial road needs to be used in the process of subarea division, this operation is generally carried out by the traffic control server in the command center.

3.1 Analyzing the correlation degree

The correlation degree is a quantitative parameter that specifies the correlation between the traffic flows of two adjacent intersections. It describes the

compatibility of the traffic status and the signal timing plans of the two adjacent intersections. Lu *et al.* (2009) found that the correlation degree depends mainly on the segment distance, the traffic flow density, and the signal cycle time of the adjacent intersections. The segment distance is a static factor that exerts a fixed influence on the correlation degree, while the other factors are dynamic and introduce a time-variant effect.

3.1.1 Influence of segment distance

Experience has shown that the longer the segment distance between two adjacent intersections, the lower the correlation degree. If the segment distance is very short, say less than 200 m, the traffic flow platoon on the segment can be maintained during its travel from one intersection to the next. In this case, the correlation degree is quite high and the signals of these two intersections can be managed well through a coordination control scheme. Conversely, if the segment distance is very long, say greater than 1200 m, the traffic flow platoon shows a relatively high degree of discreteness and instability. In this case it can be deemed that the correlation degree is zero and the implementation of a coordination control is inappropriate. Based on the above discussions, the coefficient of the influence of the segment distance F_d on the correlation degree can be calculated by

$$F_d = \begin{cases} 1, & d < 200 \text{ m}, \\ (1200 - d)/1000, & 200 \text{ m} \leq d \leq 1200 \text{ m}, \\ 0, & d > 1200 \text{ m}, \end{cases} \quad (1)$$

where d is the segment distance and $F_d \in [0, 1]$. If the segment distances between two adjacent intersections along the two traveling directions are not the same, the maximum F_d is taken.

3.1.2 Influence of traffic flow density

The traffic flow density is known to be a main factor determining whether the signals of the adjacent intersections can be put under a coordination control scheme. If the flow density is relatively low, vehicles can disperse easily and the correlation degree will be low. Conversely, if the flow density is high, it will be difficult for other vehicles to jump into the travel platoon, and the traffic flow between the adjacent

intersections will be more orderly. In this situation, the correlation degree is high; therefore, adopting a coordination control strategy could be of great benefit. The coefficient of the effect of traffic flow density F_ρ between two adjacent intersections is defined as follows:

$$\rho_{(i \rightarrow i+1)} = \frac{Q_{E(i \rightarrow i+1)} + Q_{P(i \rightarrow i+1)}}{m_{(i \rightarrow i+1)} d_{(i \rightarrow i+1)}}, \quad (2)$$

$$F_\rho = \min \left(\max \left(\frac{\rho_{(i \rightarrow i+1)}}{\rho_{s(i \rightarrow i+1)}}, \frac{\rho_{(i+1 \rightarrow i)}}{\rho_{s(i+1 \rightarrow i)}} \right), 1 \right), \quad (3)$$

where $i \rightarrow i+1$ represents the traffic flow direction from intersection i to $i+1$, $i+1 \rightarrow i$ represents the reverse direction, Q_E is the number of vehicles in passenger car units (PCU), Q_P is the predicted increment of vehicles (in PCU) in the next signal cycle time (Ren and Shen, 2010), m is the number of lanes, d is the segment distance, ρ is the traffic flow density (PCU/m) on the section, and ρ_s is the associated saturated traffic flow density. Eq. (3) indicates that the larger value of the two flow density ratios (corresponding to the two different travel directions) is taken as F_ρ , and $F_\rho \in [0, 1]$.

3.1.3 Influence of signal cycle time

According to the established traffic signal control theory, if the signals of adjacent intersections are implemented by a signal coordination control scheme, their signal cycle times must be equal or in proportional relation. Thus, the correlation degree between two adjacent intersections is low if their signal cycle times are significantly different. In contrast, if their signal cycle times are approximately equal, the resulting correlation degree is high. The coefficient F_C of the effect of signal cycle time between two adjacent intersections can be computed by

$$F_C = \left| \frac{R+1}{2} - \frac{C_b}{C_s} \right| \times \frac{2}{R-1}, \quad (4)$$

where C_b and C_s represent the larger and the smaller signal cycle time of two adjacent intersections, respectively, and R is the ratio between the maximum and the minimum cycle time, which is rarely larger

than 2. In this study, R is set to 2, and $C_b/C_s \in [1, R]$, so $F_C \in [0, 1]$.

3.2 Computing the correlation degree

In this study, the correlation degree is determined by fuzzy calculation based on the key influencing factors, and is implemented in two steps (Fig. 3). The first step is threshold judgment of the segment distance, i.e., determining whether the distance d is in the region of [200, 1200] m. If d is less than 200 m, then the correlation degree D takes the maximum value of 1. If d is more than 1200 m, then D takes the minimum value of 0. When $d \in [200, 1200]$ m, the calculation process of D needs to enter the fuzzy calculation process specified in the second step, where a fuzzy module is defined to calculate the correlation degree from the three inputs of the coefficients, F_d , F_ρ , and F_C , as discussed above.

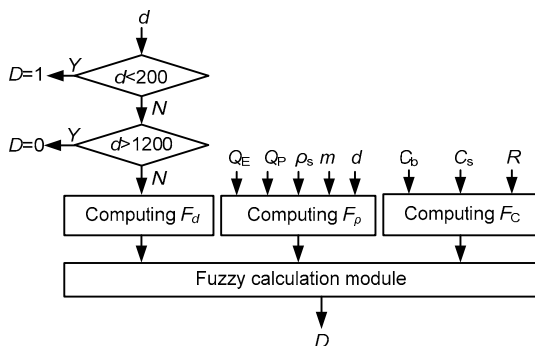


Fig. 3 Flowchart of the degree of correlation calculation

For the input variables (F_d , F_ρ , F_C) and the output D , the associated fuzzy language variables are defined as follows:

For F_d : $F_d \in [0, 1]$, and its language variables are S (small), M (medium), and B (big).

For F_ρ : $F_\rho \in [0, 1]$, and its language variables are VS (very small), S (small), LS (lightly small), LB (lightly big), B (big), and VB (very big).

For F_C : $F_C \in [0, 1]$, and its language variables are VS (very small), S (small), B (big), and VB (very big).

For D : $D \in [0, 1]$, and its language variables are VW (very weak), W (weak), M (medium), S (strong), and VS (very strong).

Fig. 4 shows the fuzzy sets defined on F_d , F_ρ , F_C , and D . The fuzzy rules are generated based on the fact that D is proportional to F_d , F_ρ , and F_C . A typical fuzzy rule takes the following form: if the segment

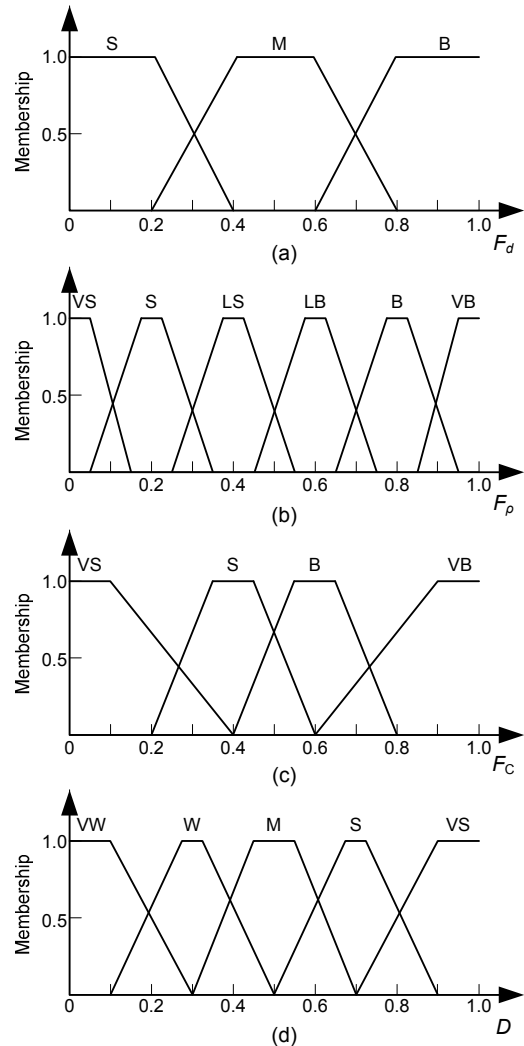


Fig. 4 The membership of fuzzy sets: (a) fuzzy sets defined on F_d ; (b) fuzzy sets defined on F_ρ ; (c) fuzzy sets defined on F_C ; (d) fuzzy sets defined on D

distance between two adjacent intersections is quite short, the traffic volume on the segment is very large, and the length of the signal cycle time of two adjacent intersections is quite the same, then the correlation degree is quite high. There are 72 fuzzy rules in total, and Table 1 lists part of the fuzzy rule base.

3.3 Dividing control areas

The division of control subareas (assigning the intersections along the arterial road into different control subareas) is based on the correlation degrees of adjacent intersections. To carry out the division process, two thresholds of the correlation degree D' and D'' (where $D' < D''$) are first chosen, for example, $D'=0.35$ and $D''=0.65$. If the correlation degree D of

Table 1 A partial list of fuzzy rules

Number	F_d	F_p	F_C	D
1	B	VS	VB	S
2	B	S	VB	VS
3	B	LS	VB	VS
4	B	LB	VB	VS
5	B	B	VB	VS
6	B	VB	VB	VS
...

S: small; VS: very small; B: big; VB: very big

any two adjacent intersections satisfies $D \leq D'$, then these two intersections must be assigned to two different control subareas, or if $D \geq D''$ then the two intersections must be assigned to the same control subarea. However, if the correlation degree D falls between the two thresholds, i.e., $D \in (D', D'')$, there is no definite rule to decide whether the two adjacent intersections should be assigned to the same control subarea, and other information, such as the actual situation of the arterial road and the intersections, may be required for the assignment. One principle in intersection assignment is that the size of the control subarea should be limited to improve the coordination effects. A reasonable assumption is that the number of intersections in a single subarea should not be more than 15. When a subarea contains too many intersections, two adjacent intersections should not be allocated into the same subarea when $D \in (D', D'')$.

Note that the thresholds D' and D'' should be chosen carefully because they affect the result of control subarea division directly. The downtown of most cities in China has a mixed traffic flow characteristic; i.e., there are many non-motor vehicles and pedestrians together with motor vehicles, which can severely disturb the progress of motor vehicles and lead to very poor traffic efficiency. A rule of thumb is that if the arterial road is located in the downtown, D' and D'' should be set relatively large. If the arterial road is in the suburbs, D' and D'' can be set smaller to improve the traffic efficiency of motor vehicles.

4 Coordination control strategies

In this section, we present the details of the proposed coordination control strategy. For urban

traffic flow, the signal phase composition has a major impact on the intersection's capacity and efficiency. For the arterial road shown in Fig. 1, to improve the throughput volume and simplify the control strategy, a three-phase configuration is proposed (Fig. 5). Phase 1 is named the up-run coordinated phase and includes the southbound traffic flow going straight, turning left, or turning right on the arterial road. Phase 2 is referred to as the down-run coordinated phase and includes the northbound traffic flow going straight, turning left, or turning right on the arterial road. Phase 3 is named the non-coordinated phase and includes all traffic flows on the east–west minor roads. If, in some particular intersections, the east–west traffic volume is not significantly smaller than that of the arterial road, phase 3 can be partitioned into two separate phases.

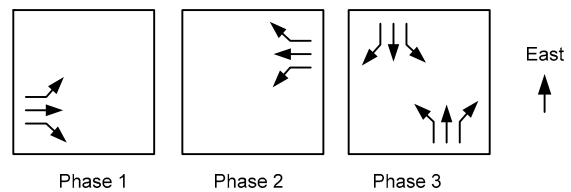


Fig. 5 Initial phase configuration

The key parameters in a coordination control strategy that need to be optimized include the common signal cycle time C of the control subarea, the split λ of each intersection, and the offset t_0 between two adjacent intersections (including the up-run and down-run directions). Phase 1's traffic flow through all the intersections in the control subarea is coordinated by the up-run offsets, while phase 2's traffic flow is coordinated by the down-run offsets. In practice, the frequency of changes in the control plan should be carefully tuned because of the effects of the build-up wave or evanescent wave generated by such changes. Too frequent changing of the control plan, e.g., once every signal cycle, will cause severe interference and flocculation of the traffic flow along the arterial road. Flocculating traffic flow can lead to unexpected traffic congestion. Therefore, a stage, which is usually equal to about eight signal cycle times, is designed so that within the stage, the control subarea, common signal cycle time, and offsets remain unchanged, while the split can be adjusted in real time at the end of each signal cycle.

4.1 Common signal cycle time

By minimizing the total vehicle delay time, the signal cycle time C_0 of each intersection in the control subarea can be computed. The Webster method given in Eq. (5) is used to determine the optimal cycle time for individual intersection (Liu, 2003):

$$C_0 = \frac{1.5L + 5}{1 - Y}, \quad (5)$$

where L is the total loss time within one signal cycle, including the yellow signal time, the lost time of the green signal, and the all-red signal time, and Y is the traffic flow ratio of the intersection calculated by

$$Y = \sum_{j=1}^p \frac{q_j}{s_j}, \quad (6)$$

where p is the total number of phases for the intersection, q_j is the traffic flow of the critical lane in phase j , and s_j is the saturation traffic flow of the critical lane in phase j . The critical lane is defined as the lane with the maximum traffic flow ratio.

After the cycle time, each individual intersection within the control subarea has been obtained, the maximum signal cycle time C_0 is taken as the common signal cycle time C for the control subarea, and the corresponding intersection is named the key intersection of the control subarea. All intersections in this subarea must adopt this common signal cycle time to obtain a coordination effect.

However, Eqs. (5) and (6) do not account for the influence of the mixed traffic flow phenomenon. To cope with interactions of motor vehicles with non-motor vehicles and pedestrians, we propose to scale up the common signal cycle time by a factor of 1.1 to 1.2 in practical applications. To reduce the computational load of the traffic control server located in the command center, we suggest that the signal cycle time C_0 for an individual intersection should be calculated within the intelligent signal controllers along the intersection road site, and then uploaded to the traffic control server in the command center. The traffic control server then compares all the cycle time requirements and determines the common signal cycle time C for the relevant control subarea, which will then be downloaded to the signal controllers.

4.2 Split and green signal time

The split and green signal times of each intersection are determined by respective traffic flow distributions in the individual intersections. The detailed calculation process is described below.

4.2.1 Calculated traffic flows in each signal cycle

To compensate for the negative effects of sudden change and random noise in traffic flow measurements on the control plan, the calculated traffic flow for phase j is introduced as follows:

$$\bar{q}_j(k) = \alpha q_j(k-1) + \beta q_j(k) + \gamma q'_j(k+1), \quad (7)$$

where $\bar{q}_j(k)$ is the calculated flow of phase j in the k th signal cycle, $q_j(k-1)$ and $q_j(k)$ are the measured traffic flows of phase j in the $(k-1)$ th and k th signal cycles, respectively, $q'_j(k+1)$ is the predicted flow of phase j in the $(k+1)$ th signal cycle (Ren and Shen, 2010), and α , β , and γ are positive weighting factors, with β controlling the real-time tracking performance while α and γ adjusting the smoothness of the calculated traffic flow. To make the calculated traffic flow consistent with the measured flow, the weighting factors are constrained by $\alpha + \beta + \gamma = 1$. In this study, $\alpha = 0.3$, $\beta = 0.5$, and $\gamma = 0.2$.

4.2.2 Split

The split is adjusted based on the calculated traffic flow described in the previous section, rather than the online traffic flow measurement. The split of phase j is determined by

$$\lambda_j = \frac{\bar{q}_j(k)}{\sum_{l=1}^3 \bar{q}_l(k)}, \quad (8)$$

where λ_j represents the split of phase j , assuming a three-phase composition (Fig. 5).

4.2.3 Green signal time

The green signal time of phase j can be calculated by

$$t_j = \lambda_j (C - t_Y - t_R), \quad (9)$$

where t_j is the green signal time of phase j , t_Y is the

total yellow signal time, and t_R is the total all-red signal time, within a signal cycle.

If $t_j < t_{j,\min}$, where $t_{j,\min}$ is the minimum green signal time for phase j , then the green signal time is set to $t_j = t_{j,\min}$. The insufficient green signal time should be supplemented by other phases proportionally, and the amount $t_{l,\text{red}}$ by which phase l needs to be reduced can be calculated by

$$t_{l,\text{red}} = \frac{\lambda_l}{\sum_{h=1,2,3; h \neq l} \lambda_h} (t_{i,\min} - t_i), \quad l = 1, 2, 3 \text{ and } l \neq i. \quad (10)$$

If $t_j > t_{j,\max}$, where $t_{j,\max}$ is the maximum green signal time of phase j , then the green signal time is set to $t_j = t_{j,\max}$. The extra green signal time should be allocated to other phases proportionally, and the amount $t_{l,\text{add}}$ by which phase l needs to be increased is determined by

$$t_{l,\text{add}} = \frac{\lambda_l}{\sum_{h=1,2,3; h \neq l} \lambda_h} (t_{i,\max} - t_i), \quad l = 1, 2, 3 \text{ and } l \neq i. \quad (11)$$

The split and the green signal time are calculated by the roadside intelligent signal controllers, and uploaded to the traffic control server located in the command center. They will be updated at the end of each signal cycle, and the new split and green signal time will be implemented in the next cycle.

4.3 Offset and start time

For two-way coordination control of the arterial road, the offset includes an up-run offset $t_o^{(i \rightarrow i+1)}$ and a down-run offset $t_o^{(i+1 \rightarrow i)}$, which are calculated by

$$\begin{cases} t_o^{(i \rightarrow i+1)} = \frac{d_{(i \rightarrow i+1)}}{v_{(i \rightarrow i+1)}}, \\ t_o^{(i+1 \rightarrow i)} = \frac{d_{(i+1 \rightarrow i)}}{v_{(i+1 \rightarrow i)}}, \end{cases} \quad (12)$$

where $i=1, 2, \dots, n-1$, n is the number of intersections within the control subarea, $d_{(i \rightarrow i+1)}$ and $v_{(i \rightarrow i+1)}$ are the segment distance and the average speed in the up-run direction from intersection i to $i+1$, respectively, and $d_{(i+1 \rightarrow i)}$ and $v_{(i+1 \rightarrow i)}$ are those in the down-run direction

from intersection $i+1$ to i , respectively. In most cases, $d_{(i \rightarrow i+1)} = d_{(i+1 \rightarrow i)}$.

To achieve the maximum benefit from coordination control, the optimal start times of phases 1 and 2 at all the intersections within the control subarea must be decided properly. We assume that the start time of phase 1 at intersection 1 in the up-run direction (referred to as t_u^1) is at the first second, and take this time as the reference point for offset coordination. The start times of phase 1 at intersection i (denoted by t_u^i) can be determined from the up-run offsets discussed in Section 3.3, using the following equation:

$$\begin{cases} t_u^1 = 1, \\ t_u^i = t_u^{i-1} + t_o^{(i-1 \rightarrow i)}, \quad i = 2, 3, \dots, n. \end{cases} \quad (13)$$

If $t_u^i > C$, then $t_u^i = t_u^i - mC$, where m is an integer which satisfies $t_u^i \in [1, C]$.

Similarly, we assume that the start time of phase 2 at intersection n in the down-run direction (referred to as t_d^n) is at time t (a variable to be optimized later). Then the start time of phase 2 at intersection i (referred to as t_d^i) can be determined from the down-run offsets through the following equation:

$$\begin{cases} t_d^n = t, \\ t_d^i = t_d^{i+1} + t_o^{(i+1 \rightarrow i)}, \quad i = n-1, \dots, 2, 1. \end{cases} \quad (14)$$

For each intersection, the start time arrangement determined by Eqs. (13) and (14) may have different configurations (Fig. 6). This is caused by the differences in the segment distance and average speed between any two adjacent intersections.

Three kinds of relationship between phases 1 and 2 are possible: (1) phases 1 and 2 are connected; (2) phases 1 and 2 overlap partially or entirely; (3) phases 1 and 2 are separated. In the first case, phase 2 starts just after phase 1 is over, and the phase sequence is 1–2–3. This is the most desirable case, but it is very unlikely in practice. In the second case, phase 2 starts before phase 1 is over. The overlap between phases 1 and 2 not only results in traffic conflicts between turning left and going straight in both phases, but also

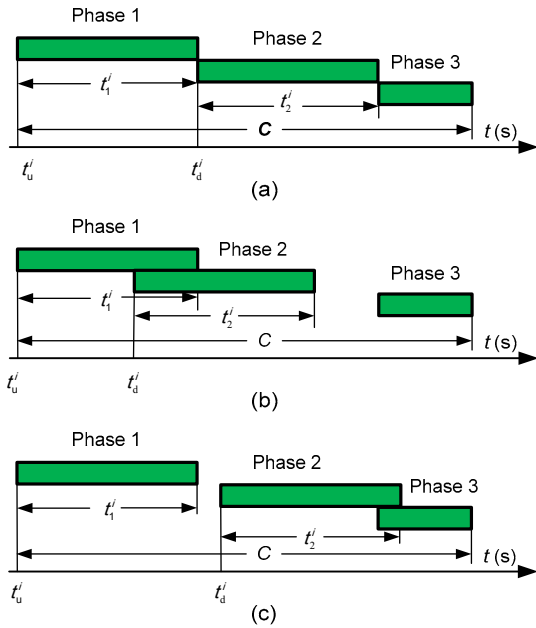


Fig. 6 Three possible configurations of the phase time series: (a) connection; (b) overlap; (c) separation

leads to extra green time. In the third case, phase 1 comes to an end before phase 2 starts, and the interval is shorter than the green time of phase 3. Thus, there is no appropriate time slot in the signal cycle to implement phase 3. The goal of the optimal control scheme is to avoid the third case, and to make the overlap time between phases 1 and 2 as small as possible when the second case occurs.

We assume that t_1^i and t_2^i are the green times of phases 1 and 2 at intersection i , respectively. Based on the above analysis, the objective for optimization is to make phases 1 and 2 of each intersection perfectly connected without overlap or separation. Considering the constraint of $t \in [1, C]$, the task of optimization is to determine the start time of phase 2 at intersection n in the down-run direction, so that the objective function J_1 , defined in Eq. (15), is minimized. The secondary objective function J_2 , defined in Eq. (16), is then maximized with t limited in the solution set of J_1 minimization.

$$J_1 = \min \left(\sum_{i=1}^n (|t_u^i - t_d^i| > a^i ? 1 : 0) \right), \quad (15)$$

$$J_2 = \max \left(\sum_{i=1}^n |t_u^i - t_d^i| \right). \quad (16)$$

In Eq. (15),

$$a^i = \begin{cases} t_1^i, & t_d^i > t_u^i, \\ t_2^i, & t_d^i < t_u^i. \end{cases}$$

With the optimal solution of t , the phase 2 start time t_d^i of other individual intersections can be calculated from Eq. (14). Again, if $t_d^i > C$, then $t_d^i = t_d^i - mC$, where m is an integer which satisfies $t_d^i \in [1, C]$.

In some practical applications, overlap or separation between phases 1 and 2 is unavoidable. In the overlapping situation, the following methods may be taken to adjust the phase time: (1) Terminate phase 1 earlier or delay the start of phase 2 to force a connected configuration from an overlapping one. However, this method may reduce the up-run or down-run green signal bandwidth. (2) Avoid traffic conflict by an early-cut-off of the left-turn signal of phase 1 and a late-release of the left-turn signal of phase 2. This is equivalent to inserting a temporary straight and right phase between phases 1 and 2 (Fig. 7). The choice of the method to adopt should be determined by the relevant road and traffic situation. In the separation situation, there are also two methods for adjusting the cycle phase configuration: (1) If the separation is large, delay the start of phase 2 appropriately and move phase 3 ahead of phase 2; (2) If the separation time is small, the phase 2 start time can be moved ahead so that phases 1 and 2 are connected without a gap. However, both methods may lead to a reduction in the bandwidth of phase 2.

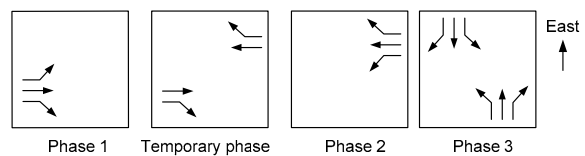


Fig. 7 Actual phase configuration

The offset and green signal start time of each phase are updated by the traffic control server in the command center and downloaded to the roadside intelligent signal controller. This process should be synchronized with the updating of the common signal cycle for the control subarea.

5 Case study

The dynamic coordination control method we developed has been implemented in several software modules, and embedded into the Traffic Control Management System (TCMS) software platform and the ACS-3 intelligent signal controller. Both TCMS and ACS-3 are products of the Zhejiang Zheda Supcon Information Co., Ltd. A dynamic traffic signal coordination control system (Fig. 8) was successfully implemented late in 2014 in Shaoxing City, Zhejiang Province, China. The control system optimizes the traffic signal control plan of the arterial Zhongxing Road, which is managed by the Shaoxing Traffic Police Department.

Zhongxing Road is a north–south arterial road running throughout Shaoxing City (Fig. 9), and plays a significant role in relieving traffic congestion and improving the city’s travel experience. The road includes a 15.90 km dual carriageway, with each carriageway having three lanes. The longest segment distance between two adjacent intersections is 1.60 km, and the shortest is 0.15 km. There are 26 intersections including 22 crossroads and 3 T-shaped intersections. The north part of this road is in the suburbs, and the south part is in the downtown area. Road traffic flows are measured using inductive loop detectors placed on each entrance lane of all intersections, and video detectors are installed on 13 key segments marked ‘*’ (Fig. 9). Fig. 10 shows the south–north going straight traffic flow data of Zhongxing Road on January 20, 2016. Using an intelligent hybrid prediction model developed by Zhejiang University (Ren and Shen, 2010), the short-term future traffic flow of the key segments can be predicted accurately. For safety considerations, appropriate speed limits are applied along the entire road, with the north section (suburban area) limited to 80 km/h, and the south section (urban area) limited to 50 km/h.

The key design parameters for the coordination control system were chosen as follows: $\rho_{s(i \rightarrow i+1)}$ and $\rho_{s(i+1 \rightarrow i)}$ in Eq. (3) were both set to 0.143 PCU/m; R in Eq. (4) was 2; $D'=0.3$ and $D''=0.6$ in the north section of the Zhongxing road, while $D'=0.4$ and $D''=0.7$ in the south; the yellow signal time and the all-red signal time in each phase in Eqs. (5) and (9) were 3 s and 2 s,

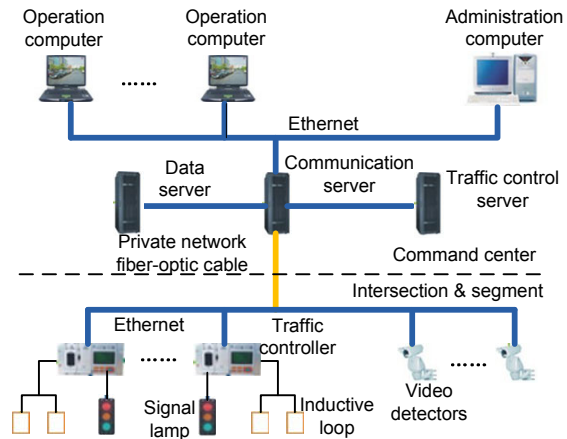


Fig. 8 Architecture of the dynamic traffic coordination control system



Fig. 9 A diagram of Zhongxing Road in Shaoxing City, Zhejiang Province, China

respectively; the lost time of green signal of each phase in Eq. (5) was 0.5 s; in Eq. (7) $\alpha=0.3, \beta=0.5$, and $\gamma=0.2$; in Eq. (10) $t_{3,\min}=15$ s, and $t_{1,\min}=t_{2,\min}=20$ s; in Eq. (11) $t_{3,\min}=50$ s, and $t_{1,\min}=t_{2,\min}=90$ s.

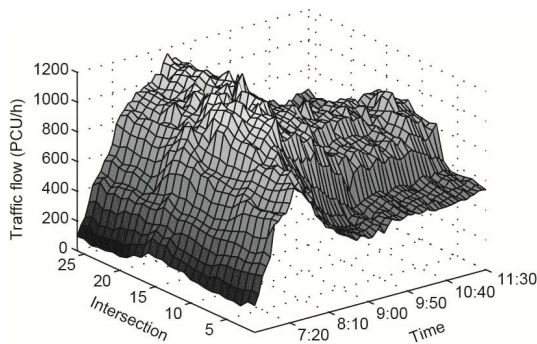
Since January 2015, this dynamic traffic coordination control system has been running smoothly. Here, two main results from 06:30 to 11:30 on January 20, 2016 are given. The dynamic division results intersections on Zhongxing Road (Fig. 9). Fig. 11 Arabic numerals represent the numbers of gives the for the control area are shown in Table 2, where the variation in the average speed of going straight vehicles on the key segments (Fig. 9).

A comparison of control performance between the proposed new method and the old method of isolated intersection adaptive control (Shen and Sun, 2002) shows a significant improvement from using the new method. The average travel time and average stop rate are the main performance indices used to evaluate the superiority of a control scheme. A statistical comparison of results obtained on January 20, 2016 and September 17, 2014, respectively, is summarized in Table 3, which confirms the superiority of the proposed method over the isolated intersection

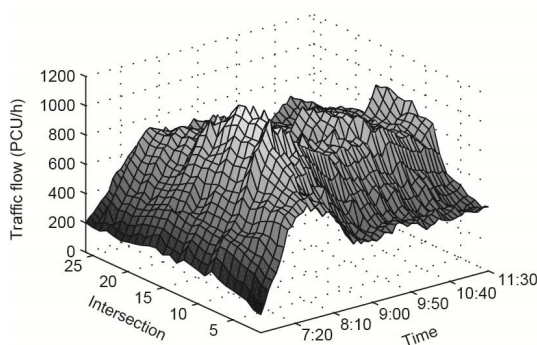
control method. A similar performance improvement can be expected if the proposed coordination control system is applied to other similar arterial roads with significant mixed traffic flow characteristics involving non-motor vehicles and pedestrian interactions.

6 Conclusions

The signal coordination control of arterial roads is an important research and engineering topic. We present a novel dynamic signal coordination control method which can dynamically assign road intersections to different control subareas, determine the common signal cycle time for each control subarea, and optimize the offset and the split based on real-time traffic conditions. The proposed control method can reduce the complexity of coordination calculations effectively, with its control performance being far superior over a static coordination control scheme or a conventional isolated intersection signal control scheme. A case study of a real traffic control scenario in Shaoxing City, Zhejiang Province, China showed very satisfactory results. We believe that the proposed

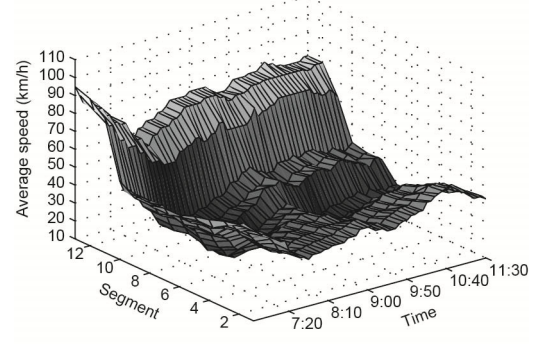


(a)

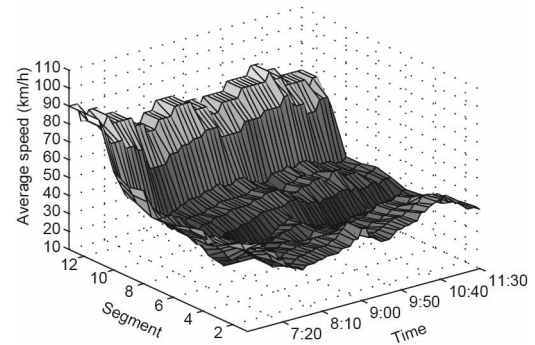


(b)

Fig. 10 The going straight traffic flow of Zhongxing Road on January 20, 2016: (a) south to north; (b) north to south



(a)



(b)

Fig. 11 The going straight average speed of vehicles on Zhongxing Road on January 20, 2016: (a) south to north; (b) north to south

Table 2 The results of dynamic division of the control area into subareas

Time	Number of intersections in each control subarea								
	No. 1	No. 2	No. 3	No. 4	No. 5	No. 6	No. 7	No. 8	No. 9
6:45	1-5	6-12	13	14-17	18	19-20	21-23	24	25-26
7:15	1-5	6-12	13-17	18	19-20	21-23	24	25-26	-
7:45	1-12	13-17	18	19-23	24	25-26	-	-	-
8:15	1-12	13-17	18	19-23	24-26	-	-	-	-
8:45	1-5	6-12	13-17	18	19-20	21-23	24-26	-	-
9:15	1-5	6-12	13-17	18	19-20	21-23	24	25-26	-
9:45	1-5	6-12	13	14-17	18	19-20	21-23	24-26	-
10:15	1-5	6-12	13-17	18	19-23	24-26	-	-	-
10:45	1-5	6-12	13	14-17	18	19-23	24-26	-	-
11:15	1-5	6-12	13	14-17	18	19-20	21-23	24	25-26

Table 3 A comparison of control performances of the old and new methods

Performance index	Direction	Time	Maximum		Minimum		Mean	
			New method	Old method	New method	Old method	New method	Old method
Average travel time (min)	South to north	Rush hour	39.2	51.3	21.7	34.5	29.1	40.4
		Peak hour	26.4	34.5	16.2	22.0	20.4	27.2
	North to south	Rush hour	37.1	47.7	19.3	30.2	26.6	39.3
		Peak hour	24.5	32.9	14.4	21.2	18.5	25.5
Average stop rate (time per car)	South to north	Rush hour	14.7	31.3	5.3	14.5	7.4	23.6
		Peak hour	8.8	26.8	4.1	9.6	5.4	14.3
	North to south	Rush hour	13.9	30.4	5.3	10.7	6.6	17.8
		Peak hour	7.8	22.2	3.9	6.1	4.5	9.8

control system is generic in nature and will find broad applications in similar arterial roads with significant mixed traffic flow characteristics.

The proposed signal coordination control method not only responds in a timely manner to the current traffic state, but also makes suitable adjustments in anticipation of future traffic state changes, with the help of an appropriate prediction model. In the developed control system, a short-term traffic flow prediction model is employed, which provides important inputs into the division of the control subareas and the coordination control module, thus further improving the coordination control performance.

Note that if the traffic flow of the arterial road is close to saturation or the traffic volume of many branches is large and close to that of the arterial road over a long period of time, the presented coordination control method might not be suitable. A new regional coordination control method needs to be developed for the control of saturated arterial roads and for road networks where all the road branches have a similar traffic flow volume.

Acknowledgements

The authors would like to thank researchers within the Department of Control Science and Engineering and the State Key Laboratory of Industrial Control Technology at Zhejiang University for their inspiring discussions and encouragement. The authors also thank the engineers within the Zhejiang Zheda Supcon Information Co., Ltd. for the engineering implementation, and the Shaoxing Traffic Police Department for providing traffic data.

References

- Febbraro, A.D., Giglio, D., Sacco, N., 2015. A deterministic and stochastic Petri net model for traffic-responsive signaling control in urban areas. *IEEE Trans. Intell. Transp. Syst.*, **17**(2):510-524.
<http://dx.doi.org/10.1109/TITS.2015.2478602>
- Gartner, N.H., Stamatiadis, C., 2004. Progression optimization featuring arterial- and route-based priority signal networks. *Intell. Transp. Syst.*, **8**(2):77-86.
<http://dx.doi.org/10.1080/15472450490437771>
- Kong, Q.J., Li, L.F., Yan, B., et al., 2013. Developing parallel control and management for urban traffic systems. *IEEE Intell. Syst.*, **28**(3):66-69.
<http://dx.doi.org/10.1109/MIS.2013.59>
- Kong, X.J., Shen, G.J., Xia, F., et al., 2011. Urban arterial traffic two-direction green wave intelligent coordination

- control technique and its application. *Int. J. Contr. Autom. Syst.*, **9**(1):60-68.
<http://dx.doi.org/10.1007/s12555-011-0108-4>
- Kumar, P., Merzouki, R., Conrard, B., et al., 2014. Multilevel modeling of the traffic dynamic. *IEEE Trans. Intell. Transp. Syst.*, **15**(3):1066-1082.
<http://dx.doi.org/10.1109/TITS.2013.2294358>
- Lee, J.H., Lee-Kwang, H., 1999. Distributed and cooperative fuzzy controllers for traffic intersections group. *IEEE Trans. Syst. Man Cybern. C*, **29**(2):263-271.
<http://dx.doi.org/10.1109/5326.760570>
- Lertworawanich, P., Kuwahara, M., Miska, M., 2011. A new multiobjective signal optimization for oversaturated networks. *IEEE Trans. Intell. Transp. Syst.*, **12**(4):967-976. <http://dx.doi.org/10.1109/TITS.2011.2125957>
- Liu, Z.Y., 2003. Intelligent Traffic Control Theory and Application. Science Public House, Beijing, China, p.22-23 (in Chinese).
- Lu, K., Xu, J.M., Zheng, S.J., 2009. Correlation degree analysis of neighboring intersections and its application. *J. South China Univ. Technol. Nat. Sci.*, **37**(11):37-42 (in Chinese).
- Pillai, R.S., Rathi, A.K., Cohen, S.L., 1998. A restricted branch-and-bound approach for generating maximum bandwidth signal timing plans for traffic networks. *Transp. Res. B-Method*, **32**(8):517-529.
[http://dx.doi.org/10.1016/S0191-2615\(96\)00033-1](http://dx.doi.org/10.1016/S0191-2615(96)00033-1)
- Ren, S.P., Shen, G.J., 2010. Intelligent hybrid forecasting technique for short-term traffic flow. *J. Zhejiang Univ. (Eng. Sci.)*, **44**(8):1473-1478 (in Chinese).
- Shen, G.J., Kong, X.J., 2009. Study on road network traffic coordination control technique with bus priority. *IEEE Trans. Syst. Man Cybern. C*, **39**(3):343-351.
<http://dx.doi.org/10.1109/TSMCC.2008.2005842>
- Shen, G.J., Sun, Y.X., 2002. Multi-phase fuzzy traffic control based on phase sequencer. *Contr. Dec.*, **17**(Suppl.): 654-658 (in Chinese).
- Tettamanti, T., Luspai, T., Kulcsár, B., et al., 2014. Robust control for urban road traffic networks. *IEEE Trans. Intell. Transp. Syst.*, **15**(1):385-398.
<http://dx.doi.org/10.1109/TITS.2013.2281666>
- Wu, W.G., Zhang, J.B., Luo, A.X., et al., 2015. Distributed mutual exclusion algorithms for intersection traffic control. *IEEE Trans. Parall. Distr. Syst.*, **26**(1):65-74.
<http://dx.doi.org/10.1109/TPDS.2013.2297097>